

SCALE-MODEL CHARGE-TRANSFER TECHNIQUE FOR MEASURING ENHANCEMENT FACTORS

J. Kositsky and J.E. Nanevich
SRI International, Menlo Park, California

ABSTRACT

Determination of aircraft electric-field enhancement factors is crucial when using airborne field mill (ABFM) systems to accurately measure electric fields aloft. SRI used the scale-model charge-transfer technique to determine enhancement factors of several canonical shapes and a scale model Learjet 36A. The measured values for the canonical shapes agreed with known analytic solutions within about 6%. The laboratory-determined enhancement factors for the aircraft were compared with those derived from in-flight data gathered by a Learjet 36A outfitted with eight field mills. The values agreed to within experimental error (~15%).

INTRODUCTION

Aerial measurements of atmospheric electric fields can provide data that are essential for accurately assessing the danger of triggered lightning to space-launch vehicles. A properly instrumented aircraft can resolve the ambient vector electric field aloft in real time and can telemeter critical data to ground personnel during a prelaunch countdown sequence. In addition, postflight analyses of stored electric-field and meteorological data can be used to study the fundamental processes of cloud electrification.

To successfully measure the ambient electric fields aloft, it is crucial to accurately quantify the perturbation of the fields by the aircraft itself. In general, an electrostatic field is perturbed by the presence of a conducting body so that the field lines terminate normal to the object's surface. The factor by which the ambient field is modified at a given point on the surface is referred to as the "enhancement" or "form" factor of that object at that point.

Several methods of determining enhancement factors have been used historically. The method described here, the scale-model charge-transfer technique, has been used with varying degrees of success since the time of Maxwell [1]. Studies at SRI International [2,3] have shown that, for various canonical shapes (spheres and prolate spheroids) with analytic solutions in closed form, this technique, when carefully performed, can provide accurate enhancement factors. The technique was also used to determine the enhancement factors of a Learjet 36A. During the latter part of July 1989, SRI modified and updated an existing ABFM system for integration with the Aeromet Learjet 36A High-Altitude Reconnaissance Platform (HARP) that had also been used for meteorological support of rocket launch and reentry tests in the Pacific. Flight experiments were performed using aircraft maneuvers with the HARP under specific field conditions near the Kennedy Space Center. These data were used to independently compute the enhancement factors at the field meter locations and verify the scale-model charge-transfer measurements.

SCALE-MODEL CHARGE-TRANSFER TECHNIQUE

The scale-model charge-transfer technique is performed in an artificially produced uniform electric field. A conductive model of an object, for which the enhancement factors are required, is suspended in this field, distorting the otherwise uniform field in the same manner as the full-scale object would distort a uniform ambient field.

The charge density at any point, i , on a conductor's surface is proportional to the electric field magnitude, E_i , at that point. In the scale-model charge-transfer technique, the electric field at the points where the enhancement factors are required is measured by sampling the charge density at those points. This is accomplished by touching a small metal probe to the points of interest and measuring the charge that transfers from the model to the probe. Since the magnitude of this charge, q_i is proportional to the field at the point probed, the enhancement factor, a_i , can be determined by dividing by the charge q_o acquired by the same probe at a reference plate where the field is maintained at the uniform field value E_o .

$$a_i = \frac{E_i}{E_o} = \frac{q_i}{q_o} \quad (1)$$

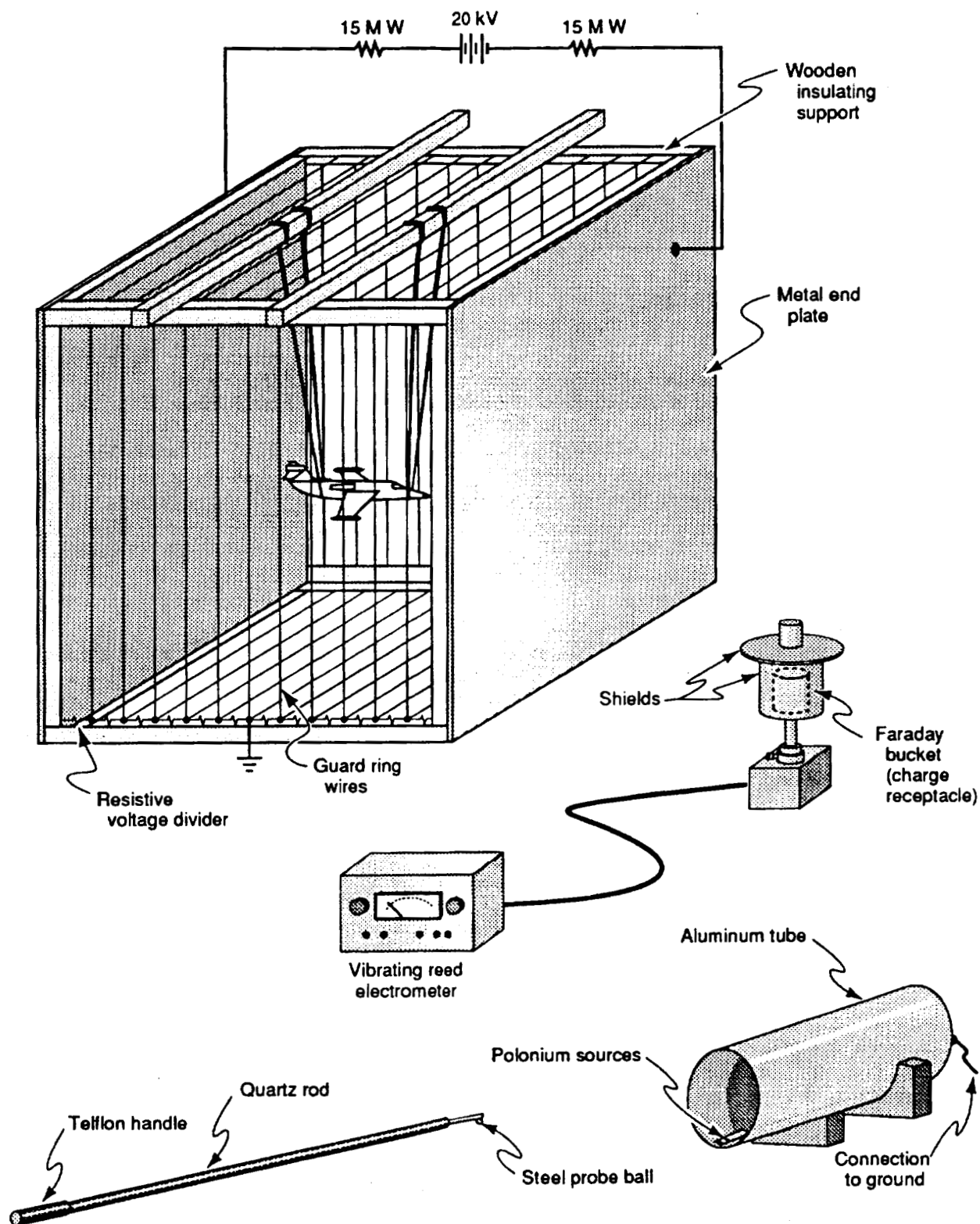
The charge on the probe is measured by bringing the charged probe into contact with the inside surface of a shielded Faraday "bucket" charge receptacle. A Cary 31 vibrating-reed electrometer, capable of measuring charges of 5×10^{-16} C, is connected to the receptacle to measure this deposited charge.

The uniform electric field was created in an electrostatic cage that consists of two large (152 cm per side) square aluminum parallel plates held 152 cm apart by a wooden frame (Figure 1). The edges of the plates are rolled over and taped to mitigate corona production. The whole frame rests on two wooden sawhorses, placed parallel to the end plates.

Electric-field fringing is minimized by a system of 15 equally spaced, insulated guard-ring wire loops held by the wooden frame parallel to the aluminum end plates. Each loop is maintained at the correct voltage to give a linear variation of potential between the plates by connecting it to a resistance voltage divider that spans the full cage voltage. Although the electric field has some fine structure near the guard wires, the field is essentially uniform over most of the cage volume.

The voltage source is an FRP-200 capable of providing 40 kV. For safety reasons, a 15 M Ω resistor is connected in series with each leg of the high-voltage supply. The voltage divider consists of fourteen 3.6 M Ω resistors, one between each pair of wire loops in the guard ring, and two 1.8 M Ω resistors for the half-width sections between the end loops and the end plates.

The high-voltage supply to the cage end plates is activated by an operator foot switch through a pair of high-voltage vacuum relays. In operation, the probe tip is touched to the correct spot on the suspended model, the relay is activated, the probe is removed from contact with the model, the relay is deactivated, and the charge on the probe is placed in the electrometer Faraday bucket.



p91-003/11

Figure 1 ELECTROSTATIC CAGE SCALE-MODEL CHARGE-TRANSFER APPARATUS

The probe is a 3 mm (1/8 inch) diameter steel ball fastened to the tapered end of a 50 mm (2 inches) long Teflon rod. The Teflon rod, which is about 3 mm (1/8 inch) in diameter, is inserted into one end of a hollow quartz rod about 1 m (40 inches) in length that is insulated from the experimenter by a 15 cm (6 inches) Teflon handle (Figure 1).

Experiments were performed with the probes to check for charge buildup and leakage by varying the time between probing the model and depositing the charge in the Faraday bucket. No leakage or buildup effects were noted for delay times of up to 5 minutes. Typically, only 5 to 10 seconds are needed to transfer the charge to the electrometer bucket.

Several 500 μCi polonium sources were placed inside a 15 cm (6 inches) diameter metal grounded tube, thus producing a field-free ionized region. Before taking a measurement, stray charges that might collect on the probe's dielectric surfaces are neutralized by passing the probe over the polonium sources.

An accurate conductive scale model of the aircraft (or other object) is suspended near the center of the cage by waxed nylon thread tied to wooden slats placed on top of the frame parallel to the equipotentials. The thread, as well as the insulated guard rings, are neutralized by passing polonium sources along their lengths. The model is oriented in turn with its x, y, and z axes parallel to the applied electric field. This allows the enhancement factors a_x , a_y and a_z , due to electric-field components E_x , E_y and E_z respectively, to be measured independently. The model is momentarily grounded before the measurements to ensure that it is electrically neutral.

The field enhancement at the points where field mills are located is determined by measuring a quantity proportional to the charge density, and therefore the electric field, at these points using the small metal probe, as outlined above. The electrostatic cage end plates are then similarly sampled to obtain a quantity proportional to the ambient field in the cage. The enhancement factors are equal to the ratio of these measurements as shown in Eq. 1.

This procedure is repeated with the aircraft model suspended in the cage in three orthogonal positions relative to the applied electric field to obtain the enhancement factors, a_{1x} , a_{1y} , and a_{1z} . To obtain the coefficients, a_{1v} , quantities analogous to enhancement factors that give the field at point i due to charge buildup on the airframe, a similar procedure is followed with the model suspended in a field-free region ($E_x = E_y = E_z = 0$). The model is charged to a known potential and probed at the same field mill sites. In this case, however, the results must be divided by the scaling factor of the scale model to obtain a_{1v} .

CANONICAL SHAPE EXPERIMENTS

Several solids have shapes that allow the enhancement factors to be computed in closed form directly from Maxwell's equations. Experiments with several of these shapes (spheres and various prolate spheroids) were performed to test the experimentally derived enhancement factors against the theoretical values. The results of these experiments (described below) show that the absolute uncertainty of the enhancement factors calculated from the scale-model charge-transfer technique data are within approximately 6% (including systematic errors).

A 130 mm (5 inches) diameter aluminum sphere and two aluminum prolate spheroids with axis ratios of 2 and 5 and major axes of 200 mm and 300 mm,

respectively, were machined. Each solid was carefully marked to divide the semimajor axis into ten equal segments. A freshly cleaned 6 mm (1/4 inch) dot punched from copper tape was centered on the marks. These dots acted as targets for the experimenter to probe and also nullified most of the contact potential effect, since the Faraday bucket was also made of copper.

The results of the experiments (plotted points) and theoretical curves (lines) for the sphere and the prolate spheroids of axis ratio $c/b = 2$ with major axis aligned perpendicular to the field are shown in Figures 2a. Figure 2b shows the results for the prolate spheroids of axis ratios $c/b = 2$ and $c/b = 5$ with major axes parallel to the field. In these figures, the models are assumed to be at the center of a rectangular coordinate system. The enhancement factors are shown for points on the model surface as a function of relative position in the z-direction, though (except for the end point) not on the z-axis itself. Even at the spheroid tips, which have small radii of curvature (a place field mills are not normally located), the experimental results presented in all the curves are in close agreement with theory.

Field-free measurements ($E = 0$) were taken on the prolate spheroid of axis ratio 5 raised to a potential of 1300 V by means of a suspending wire. Image charge problems were minimized by suspending the model about 1.5 m (5 ft) from any other object. As shown in Figure 3, the agreement between the measured and the theoretically calculated values is better in the lower half of the prolate and diminishes as points approach the wire. This is to be expected, since the wire, being of the same polarity as the model, causes like charge to migrate from proximal to distal regions on the suspended model. The perturbation effect observed is, of course, greater at points closer to the perturbation source, the wire. Nonetheless, the results indicate that, as long as the wire to the model is kept on the side opposite the points probed, the results (including systematic errors) are typically within 6%.

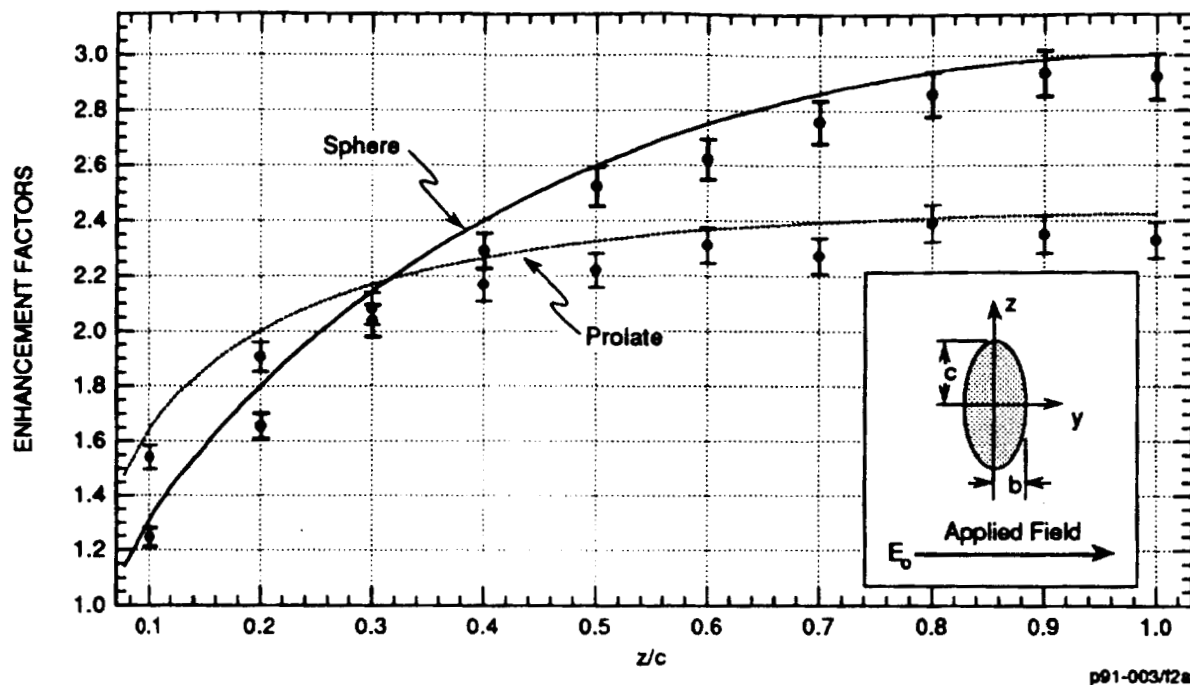
Figures 2 and 3 show that almost all the experimentally derived values are less (by about 6%) than the theoretical values, which indicates a small systematic error in the technique. A similar systematic error was reported by Rudolph et al. [4]. Even with this error, the agreement between the measured and the theoretical values of the enhancement factors, indicative of the absolute accuracy of this technique, is excellent.

LEARJET 36A MODEL MEASUREMENTS

A 1:36 scale model of a Learjet 36A was spray-painted with silver conductive paint. After testing the conductivity with an ohmmeter, the locations of the field mills were carefully marked. The model was suspended at the center of the electrostatic cage and aligned in turn to each of the three Cartesian coordinates defined by the cage axes. After determining the enhancement factors, a_{1x} , a_{1y} , and a_{1z} , the model was suspended in a field-free region and raised to a potential of 1300 V to obtain the a_{1v} .

Eight electric field mills were installed on a Learjet 36A at locations corresponding to the points probed on the scale model. The in-flight data from 18 deployments at Kennedy Space Center during August and September 1989 were used to check the laboratory-derived enhancement factors. The results from two of the many techniques that were used to verify the enhancement factors [3] are presented here.

a. Sphere and prolate spheroid ($c/b = 2$) with major axis perpendicular to field



b. Prolate spheroids ($c/b = 2$, $c/b = 5$) with major axes parallel to field

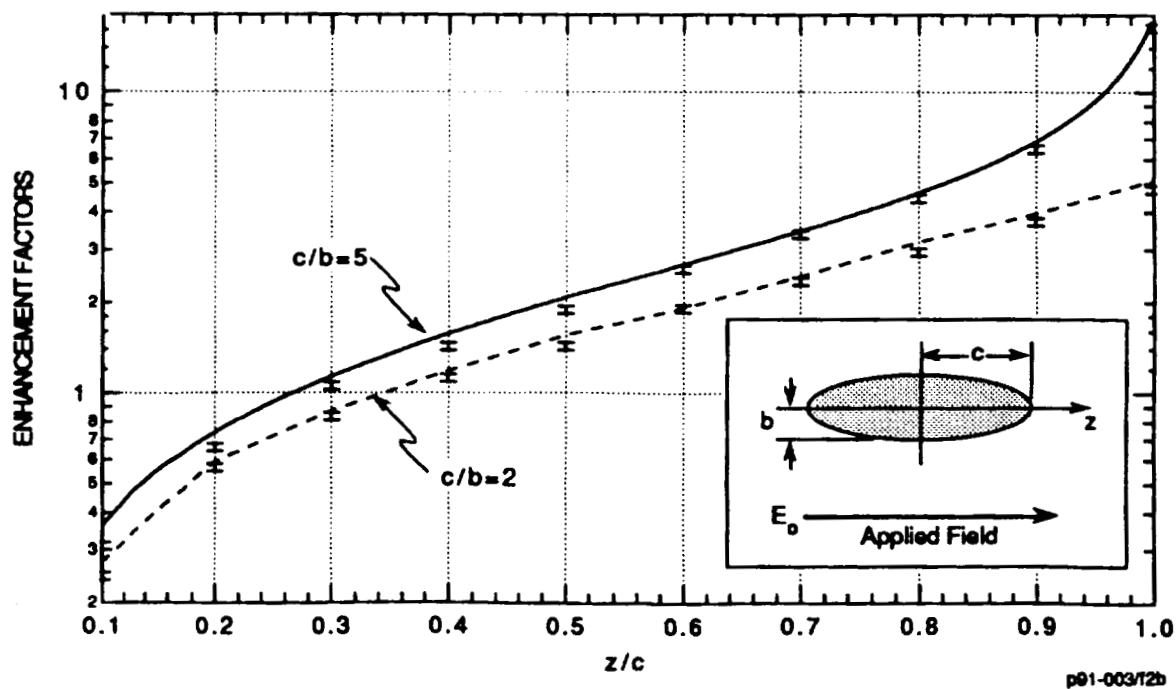


Figure 2 THEORETICAL CURVES AND EXPERIMENTAL DATA OF ENHANCEMENT FACTORS

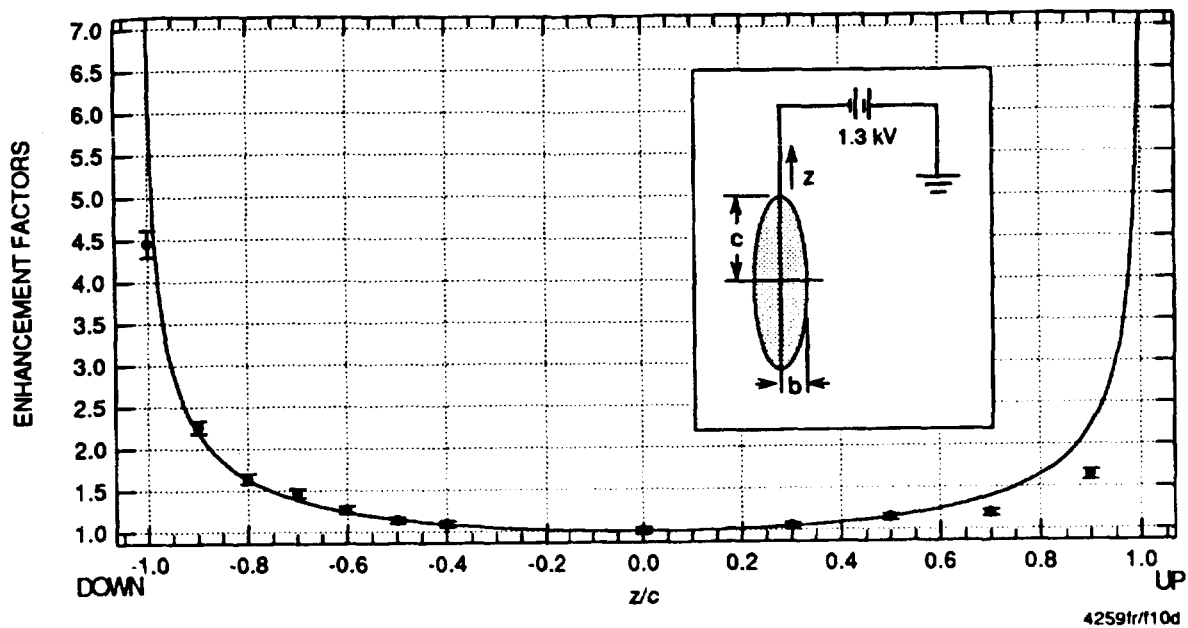


Figure 3 THEORETICAL CURVE AND EXPERIMENTAL DATA OF ENHANCEMENT FACTORS FOR A CHARGED PROLATE SPHEROID $c/b = 5$, SUSPENDED BY A WIRE IN A FIELD-FREE REGION

During fair weather (very low ambient field conditions), the aircraft was artificially charged to high potentials via a corona discharge point. The field-mill output data due to this self-charging were used to calculate the ratios of the electric potential enhancement factors, a_{iv} . The results from experiments performed on six different days show excellent agreement between the laboratory-measured and the in-flight-data-derived enhancement factors. Table I shows that the results are well within experimental error, with an average difference of only 1%.

Table I

COMPARISON OF LABORATORY AND IN-FLIGHT-DATA-DERIVED ENHANCEMENT FACTORS DURING ARTIFICIAL CHARGING EXPERIMENTS IN CLEAR AIR

Enhancement Factor Ratio	Laboratory-Derived Ratio	In-Flight Data-Derived Ratio	Difference
a_{1v}/a_{3v}	1.08 ± 0.03	1.07 ± 0.02	1%
a_{2v}/a_{3v}	1.01 ± 0.03	1.01 ± 0.03	0%
a_{4v}/a_{3v}	1.00 ± 0.03	1.01 ± 0.02	1%
a_{5v}/a_{3v}	0.62 ± 0.02	0.61 ± 0.01	2%
a_{6v}/a_{3v}	0.93 ± 0.03	0.93 ± 0.03	0%
a_{7v}/a_{3v}	0.62 ± 0.02	0.62 ± 0.02	0%

Data were collected during aircraft roll and pitch maneuvers during periods of strong vertical fields (at low altitudes over the ocean under a large thunderstorm system). These data were used to calculate several enhancement factor ratios, which are compared with the laboratory-derived enhancement factors in Tables II and III.

Table II

COMPARISON OF Z-COMPONENT ENHANCEMENT FACTORS FROM
SCALE-MODEL CHARGE-TRANSFER MEASUREMENTS AND IN-FLIGHT DATA
DURING ROLL MANEUVERS

Enhancement Factor Ratios	Charge- Transfer	In-Flight Data	Difference
a_{1z}/a_{3y}	1.47 ± 0.03	1.73 ± 0.17	18%
a_{2z}/a_{3y}	-1.47 ± 0.03	-1.21 ± 0.13	18%
a_{5z}/a_{3y}	1.16 ± 0.03	1.13 ± 0.10	3%
a_{6z}/a_{3y}	-1.37 ± 0.03	-1.46 ± 0.15	7%

Two pairs of ratios in Table II agree within one error bar, while the remaining two pairs of ratios agree to within two error bars. The agreement is not as good as it might be because uncertainties in the in-flight ratios were underestimated. These uncertainties were calculated while ignoring the errors introduced by the assumptions of a purely vertical field and perfectly performed maneuvers (i.e., roll maneuvers with zero pitch and vice versa). Even with these underestimated uncertainties (median of 10%) in the in-flight ratios, the ratios from the scale-model charge-transfer technique have even smaller computed uncertainties (median of 2%).

Table III

COMPARISON OF X-COMPONENT ENHANCEMENT FACTORS FROM
SCALE-MODEL CHARGE-TRANSFER MEASUREMENTS AND IN-FLIGHT DATA
DURING PITCH MANEUVERS

Enhancement Factor Ratios	Charge- Transfer	In-Flight Data	Difference
a_{1x}/a_{3x}	1.00 ± 0.03	0.89 ± 0.10	11%
a_{2x}/a_{3x}	0.93 ± 0.03	0.81 ± 0.12	13%
a_{4x}/a_{3x}	1.00 ± 0.03	1.01 ± 0.09	1%
a_{5x}/a_{3x}	-0.01 ± 0.02	-0.27 ± 0.15	-
a_{6x}/a_{3x}	-0.62 ± 0.02	-0.37 ± 0.08	40%
a_{7x}/a_{3x}	0.46 ± 0.02	0.47 ± 0.05	2%

Four of the six pairs of ratios in Table III agree within one error bar, and one pair agrees within two error bars. As in Table II, the uncertainties in the in-flight ratios (median of 19%) are underestimates, but still larger than the uncertainties in the ratios from the scale-model charge-transfer technique (median of 3%). The large percent standard deviations for the ratio a_{5x}/a_{3x} are due to the small absolute values of the ratios themselves. Because the percent standard deviations in this ratio themselves are so large, the percent difference is not a meaningful quantity and was omitted.

The uncertainties shown for the in-flight data potential ratios (Table I) are much smaller than the errors shown for ratios computed during maneuvers (Tables II and III). For several reasons, measurements made during aircraft maneuvers are inherently more difficult and less accurate. The uncertainties in enhancement factors calculated by the scale-model charge-transfer technique are generally several times smaller than the uncertainties in the in-flight data-derived enhancement factors.

SYSTEMATIC ERRORS

Although the scale-model charge-transfer technique is excellent for measuring enhancement factors, care must be taken in designing and performing the experiments. Many details, if overlooked, can lead to errors that substantially degrade the results. Some of these concerns are discussed below.

Contact potential errors can result from the use of dissimilar metals for the model, probe, and charge receptacle. To counteract contact potential effects, three strategies are simultaneously adopted: (a) The spots on the cage end-plate and the model that are to be probed are marked by copper tape to match the copper Faraday bucket of the electrometer; (b) the polarity of the field is reversed and the results averaged; and (c) the highest voltages possible (without producing corona) are selected to increase the induced charge on the model and thus decrease the ratio of contact potential effect to induced charge effect.

The electrically polarized model in the electrostatic cage will cause a redistribution of charge on the cage end plates. The resulting image charging will affect the magnitude and uniformity of the field within the cage. A given level of acceptable image charge perturbation constrains the size of the model that can be used in a given electrostatic cage. A detailed calculation of the image charge effect for our setup indicated a very small image charge effect ($< 1\%$) on the field in the cage.

Probe perturbation errors result from the finite-sized spherical probe interacting with the model in the electric field. An analytic solution was found for the problem of two uncharged, touching conducting spheres of different radii in a uniform electric field [5]. This solution gives the correction factors by which the raw data need to be divided to account for probe perturbation on a sphere. These correction factors can also be used to estimate the probe interaction with more complex shapes, as long as the probe is small and the point probed is convex. This is accomplished by estimating the "radius of curvature" of the model at the points probed. This method gives good results, since the correction terms are a weak function of the radius of curvature of the surface probed and, except for "sharp" spots on the model, typically range between 0.95 and 0.99.

CONCLUSIONS

When carefully performed with a small probe, the scale-model charge-transfer technique accurately determines enhancement factors. Comparisons with analytic solutions for spheres and prolate spheroids show the high accuracy of the charge-transfer technique for simple canonical shapes. Comparisons with the results from methods of determining and testing enhancement factors from in-flight data (more of which can be found in [3]), also demonstrate the high accuracy of this technique on complex bodies.

ACKNOWLEDGMENTS

Part of the work reported here was supported by the Air Force Space Systems Division under contract F04701-90-C-0023.

The authors would like to thank Major M. Jeane and Captain M. Johnson, as well as Dr. K. Moe, Major J. Bassi, Dr. S. Book, J. Brinkley and H. Heritage for their helpful input and management. R. Harris-Hobbs, L. Rose and many others at Aeromet, Inc. were indispensable partners in the Learjet experiments. K. Giori, R. Maffione, and P. Sechi were among the many people at SRI who have contributed heavily in the continuing work on electric field measurements aloft.

REFERENCES

- 1 J. C. Maxwell, A Treatise on Electricity and Magnetism, Vol. 1, Article 175, Dover Publications, Inc., New York, 1891.
- 2 R. A. Maffione, J. Kositsky, K. L. Giori, and J. S. Thayer, "Aerial Measurements of Electric Fields Aloft: Flight Report, System Calibration and Accuracy," Final Report, Project 4259, SRI International, Menlo Park, California, 1989.
- 3 J. Kositsky, K. L. Giori, R. A. Maffione, D. H. Cronin, and J. E. Nanevich, "Airborne Field Mill (ABFM) System Calibration Report," Task A, Final Report, Project 1449, SRI International, Menlo Park, California, January 1991.
- 4 T. H. Rudolph, J. Horenbala, F. J. Eriksen, H. W. Weigel, J. R. Elliott, S. L. Parker, and R. A. Perala, "Interpretation of F106B and CV580 In-Flight Lightning Data and Form Factor Determination," NASA Contractor Report 4250, Contract NAS1-17748, September 1989.
- 5 J. Latham and B. J. Mason, "Electrical Charging of Hail Pellets in a Polarizing Electric Field," Proc. Roy. Soc., London, A266, pp. 387-401, 1962.